Supporting Information

Carbonates (Bicarbonates)/Reduced Graphene Oxide as Anode Materials for Sodium-Ion Batteries

Xin Gu,[a] Chunliu Yan,[a] Liting Yan,[a] Lei Cao,[a] Feier Niu,[b] Dandan Liu,[a] Pengcheng Dai,[a] Liangjun Li,[a] Jian Yang,[b] and Xuebo Zhao,*[a]*

[a] Research Center of New Energy Science and Technology, Research Institute of Unconventional Oil & Gas and Renewable Energy, China University of Petroleum (East China), Qingdao, 266580, P. R. China. E-mail: zhaoxuebo@upc.edu.cn

[b] Key Laboratory of Colloid and Interface Chemistry, Ministry of Education, School of Chemistry and Chemical Engineering, Shandong University, Jinan, 250100, P. R. China. E-mail: yangjian@sdu.edu.cn

Experimental Section

Sample synthesis. For the synthesis of reduced graphene oxide anchored $FeCO_3$ composite ($FeCO_3$/rGO), a certain amount of graphene oxide solution (3 wt.‰), $FeSO_4 \cdot 7H_2O$ (1.0 mmol) and ascorbic acid (0.2 g) were firstly dissolved in deionized water (30 mL). Secondly, 10 mL of $(NH_4)_2CO_3$ solution (0.5 mol L^{-1}) was added into the above solution under continuous stirring at room temperature. After stirred for 15 min, the solution was transferred into a Teflon-lined autoclave and heated to 160 ^oC for 15 h. The resulting product of $FeCO_3$/rGO was collected by filtering, washing with deionized water and ethanol, and drying under vacuum at 60 ^oC for 12 h. Following the same procedure, $CoCO_3$/rGO and $Ni(HCO_3)_2$/rGO composites were produced by replacing $FeSO_4 \cdot 7H_2O$ with $Co(CH_3COO)_2 \cdot 4H_2O$ and $Ni(CH_3COO)_2 \cdot 4H_2O$, respectively. Pure $FeCO_3$, $CoCO_3$ and $Ni(HCO_3)_2$ particles were prepared without graphene oxide and ascorbic acid in the protocol.

Sample characterization. X-ray diffraction (XRD) patterns were recorded by an X-ray diffractometer (Bruker D8 Adv.), using Cu-Kα line as a radiation source. Thermal gravimetric (TG) analysis was performed on a thermal analyzer (Netzsch TG/209F3) in air, using a heating rate of 10 ^oC min^{-1}. X-ray photoelectron spectra (XPS) were collected with an X-ray photoelectron spectrometer (Escalab 250Xi). Scanning electron microscope (SEM) images were achieved on a field emission scanning electron microscope (JSM 6700F). Transmission electron microscope (TEM) images were obtained on a transmission electron microscope (FEI Tecnai G2 F20).

Electrochemical Measurements. The working electrode was prepared by 80 wt.% active materials, 10 wt.% super P and 10 wt.% sodium carboxymethylcellulose (CMC). With the assistance of little water, the above materials were made into slurry, coated on copper foil

and dried under vacuum at 80 ^{o}C for 12 h. The typical mass loading of active material was about 1.5 mg cm^{-2}. A coin-type cell of CR 2032 was assembled in a vacuum glove box, using sodium foil as the counter electrode, glass fiber as the separator and 1 mol L^{-1} $NaClO_4$ in EC/DMC (volume ratio, 1:1) with 2 wt.% fluoroethylene carbonate (FEC) as the electrolyte. CV profiles were obtained from an electrochemical workstation (CHI760E, China) in the range of 0.01-3.0 V (vs. Na/Na^+) at a scanning rate of 0.1 mV s^{-1}. Galvanostatic charge/discharge measurements were performed at 0.01-3.0 V (vs. Na/Na^+) at the current densities of 50-2000 mA g^{-1} at room temperature on a battery cycler (LAND CT-2001A, China). AC electrochemical impedance spectra (EIS) were acquired on an electrochemical workstation (CHI760E, China) in the frequency range from 0.1 MHz to 0.01 Hz.

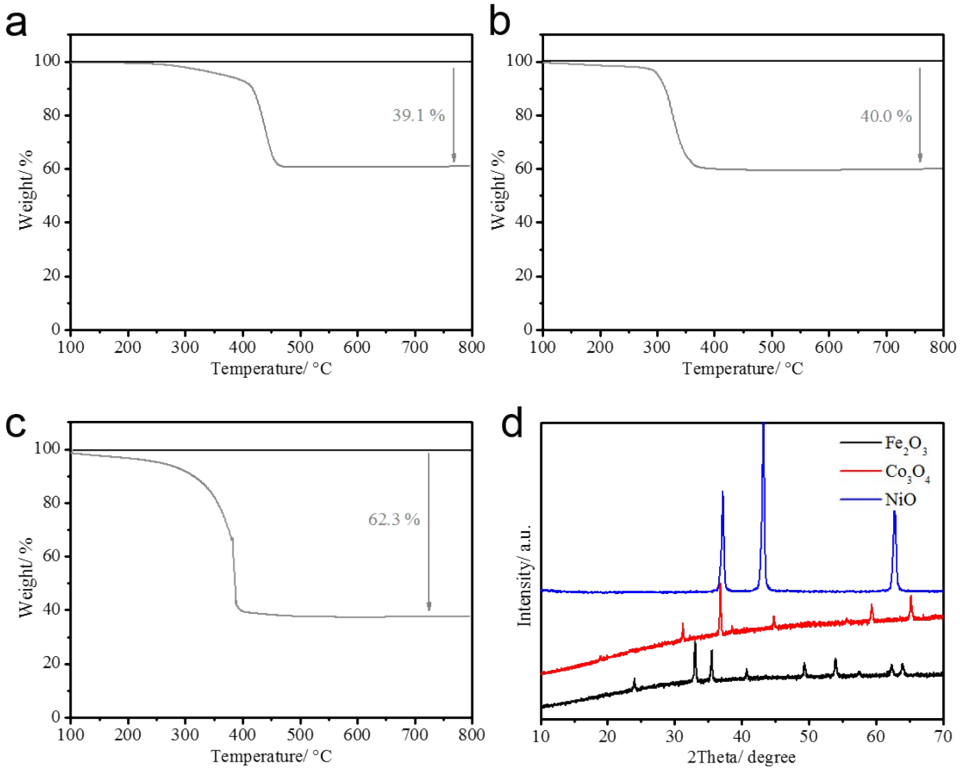

Figure S1 TG curves of (a) $FeCO_3$/rGO, (b) $CoCO_3$/rGO, and (c) $Ni(HCO_3)_2$/rGO at a heating rate of 10 ºC min^{-1} in air. (d) XRD patterns of the products obtained from annealing $FeCO_3$/rGO, $CoCO_3$/rGO and $Ni(HCO_3)_2$/rGO at 600 ºC in air for 2 h.

The carbon contents in the three rGO-modified carbonates were estimated by thermal analysis in air. As shown in Fig. S1a-c, the TG curves of $FeCO_3$/rGO, $CoCO_3$/rGO and $Ni(HCO_3)_2$/rGO powders show weight losses of 39.1 wt%, 40.0 wt% and 62.3 wt%, respectively. As confirmed by XRD data (Fig. S1d), the final products after the calcination of $FeCO_3$/rGO, $CoCO_3$/rGO and $Ni(HCO_3)_2$/rGO are Fe_2O_3, Co_3O_4 and NiO, respectively. Thus, the carbon contents in the composites are calculated to be 11.7 wt.%, 11.2 wt.% and 9.1 wt.%, respectively.

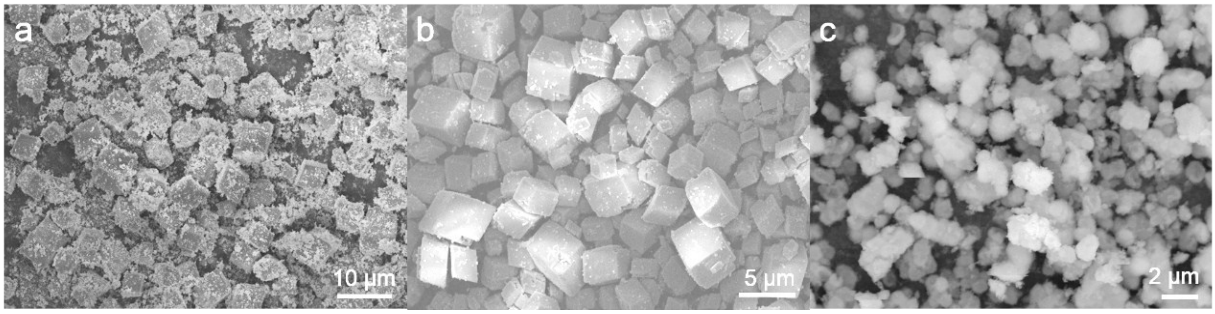

Figure S2 SEM images of (a) $FeCO_3$, (b) $CoCO_3$, (c) $Ni(HCO_3)_2$.

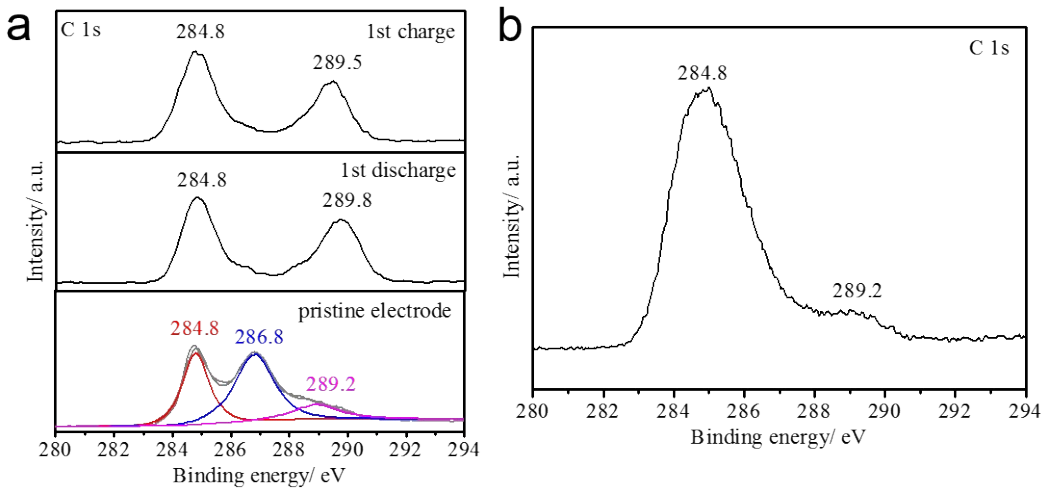

Figure S3 (a) XPS spectra of C 1s for $FeCO_3$/rGO electrode at different sodiated and desodiated states in the first cycle at the current density of 50 mA g^{-1}, (b) C 1s XPS spectrum for $FeCO_3$/rGO powder.

Figure S3a shows the C 1s XPS spectra of $FeCO_3$/rGO electrode in the first cycle. For pristine electrode, three C 1s peaks at the binding energies of 284.8, 286.8, and 289.2 eV can be assigned to C−C, C−O/C=O and CO_3^{2-}, respectively. (L. Su, Z. Zhou, X. Qin, Q. Tang, D. Wu, P. Shen, Nano Energy 2013, 2, 276-282) Compared with the C 1s spectrum of $FeCO_3$/rGO powder (Figure S3b), the C−O/C=O binding in pristine $FeCO_3$/rGO electrode is supposed to be from the sodium carboxymethylcellulose binder for making electrode. The C−O/C=O binding is disappeared after the 1st discharge process, indicating the irreversible reduction by Na^+. In addition, no obvious changes can be observed for C−C and CO_3^{2-} bindings during the discharge-charge process, indicating there is no reversible evolution of CO_3^{2-} during the electrochemical process, which is totally different from the $FeCO_3$ electrode in LIBs.

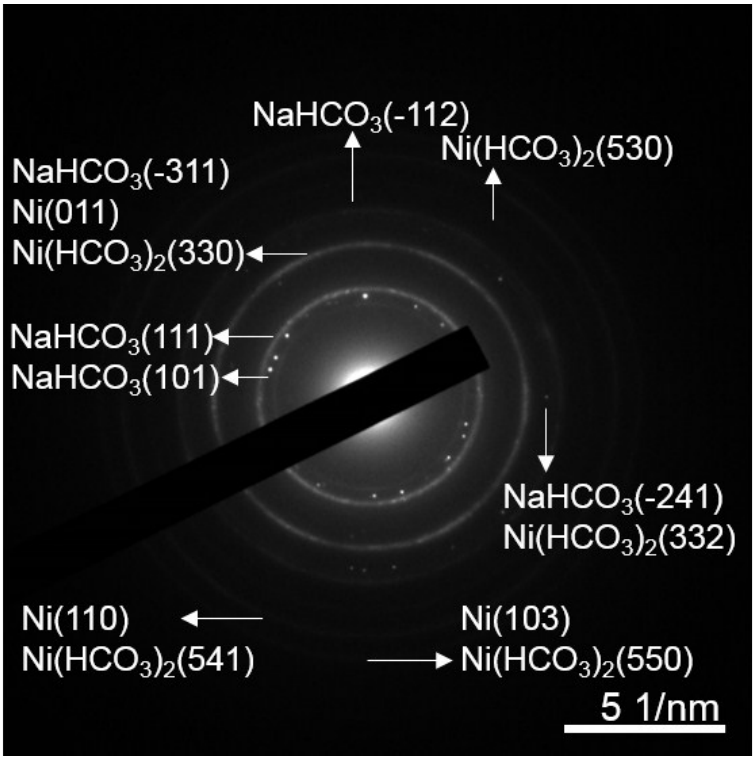

Figure S4 SAED pattern for $Ni(HCO_3)_2$/rGO electrode discharged to 0.01 V in the first cycle at the current density of 50 mA g^{-1}.

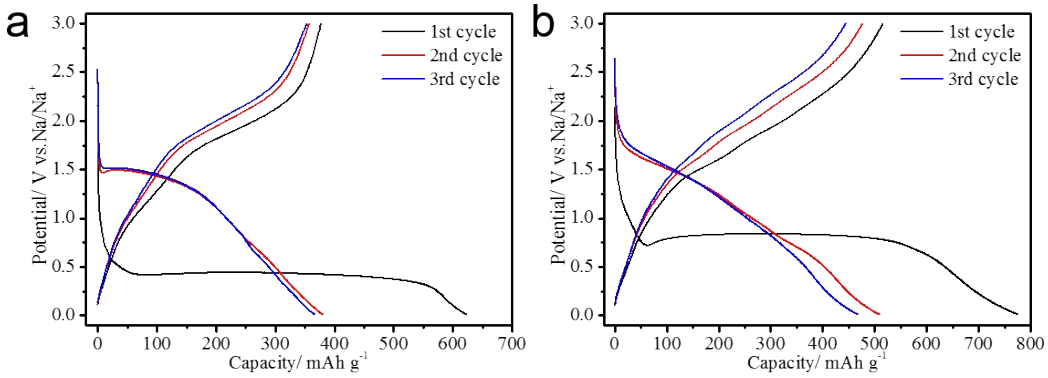

Figure S5 The first three discharge/charge curves of (a) $CoCO_3$/rGO, (b) $Ni(HCO_3)_2$/rGO electrodes at the current density of 100 mA g^{-1}.

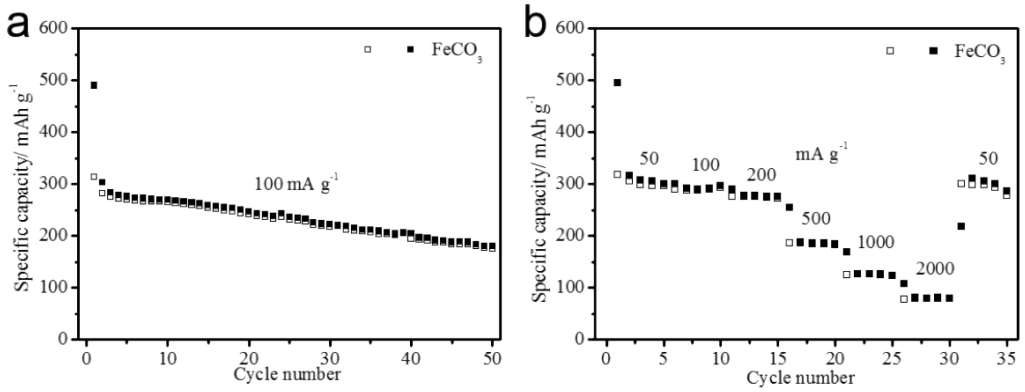

Figure S6 (a) Cycling performances and (b) rate performances of $FeCO_3$.

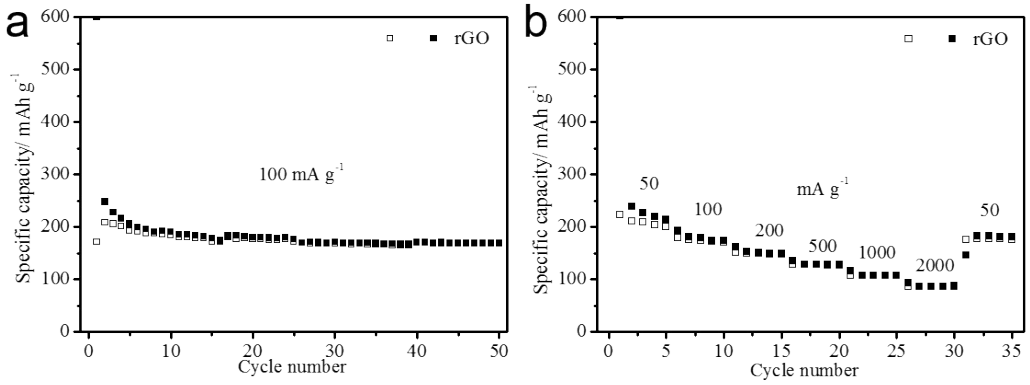

Figure S7 (a) Cycling performances and (b) rate performances of rGO.

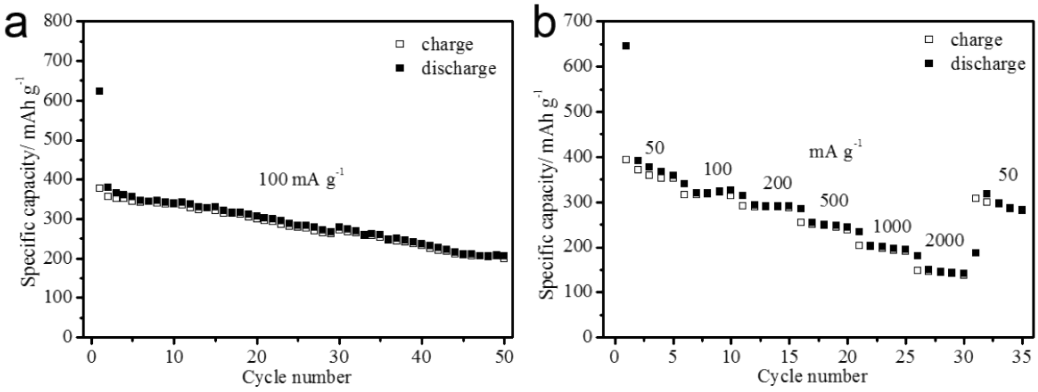

Figure S8 (a) Cycling performance of $CoCO_3$/rGO electrode at the current density of 100 mA g^{-1}. (b) Rate performance of $CoCO_3$/rGO electrode tested at the current densities of 50, 100, 200, 500, 1000, 2000 and 50 mA g^{-1} for five cycles each.

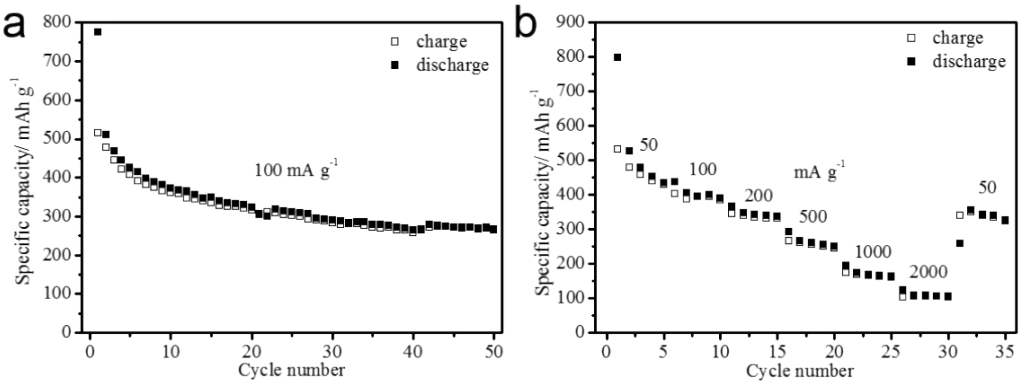

Figure S9 (a) Cycling performance of $Ni(HCO_3)_2$/rGO electrode at the current density of 100 mA g^{-1}. (b) Rate performance of $Ni(HCO_3)_2$/rGO electrode tested at the current densities of 50, 100, 200, 500, 1000, 2000 and 50 mA g^{-1} for five cycles each.

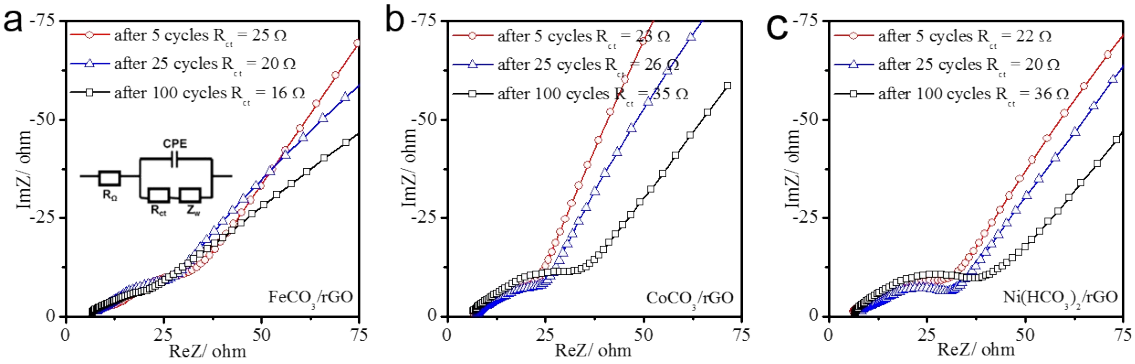

Figure S10 Nyquist plots of electrochemical impedance spectra for (a) $FeCO_3$/rGO, (b) $CoCO_3$/rGO, (c) $Ni(HCO_3)_2$/rGO electrodes after different cycles at 500 mA g^{-1}.